AIP | Applied Physics Letters

Room temperature skyrmion ground state stabilized through interlayer exchange coupling

Gong Chen, Arantzazu Mascaraque, Alpha T. N'Diaye, and Andreas K. Schmid

Citation: Applied Physics Letters **106**, 242404 (2015); doi: 10.1063/1.4922726
View online: http://dx.doi.org/10.1063/1.4922726
View Table of Contents: http://scitation.aip.org/content/aip/journal/apl/106/24?ver=pdfcov
Published by the AIP Publishing

APPLIED PHYSICS LETTERS **106**, 242404 (2015)

Room temperature skyrmion ground state stabilized through interlayer exchange coupling

Gong Chen,[1,a)] Arantzazu Mascaraque,[2,3] Alpha T. N'Diaye,[4] and Andreas K. Schmid[1]
[1]*NCEM, Molecular Foundry, Lawrence Berkeley National Laboratory, Berkeley, California 94720, USA*
[2]*Depto. Física de Materiales, Universidad Complutense de Madrid, 28040 Madrid, Spain*
[3]*Unidad Asociada IQFR (CSIC) - UCM, 28040 Madrid, Spain*
[4]*Advanced Light Source, Lawrence Berkeley National Laboratory, Berkeley, California 94720, USA*

(Received 6 April 2015; accepted 6 June 2015; published online 17 June 2015)

Possible magnetic skyrmion device applications motivate the search for structures that extend the stability of skyrmion spin textures to ambient temperature. Here, we demonstrate an experimental approach to stabilize a room temperature skyrmion ground state in chiral magnetic films via exchange coupling across non-magnetic spacer layers. Using spin polarized low-energy electron microscopy to measure all three Cartesian components of the magnetization vector, we image the spin textures in Fe/Ni films. We show how tuning the thickness of a copper spacer layer between chiral Fe/Ni films and perpendicularly magnetized Ni layers permits stabilization of a chiral stripe phase, a skyrmion phase, and a single domain phase. This strategy to stabilize skyrmion ground states can be extended to other magnetic thin film systems and may be useful for designing skyrmion based spintronics devices. © *2015 AIP Publishing LLC*. [http://dx.doi.org/10.1063/1.4922726]

Magnetic skyrmions,[1–3] nanometer-sized chiral spin objects, are of great interest in the field of spintronics because of their topological properties such as topological Hall effects[4] and current-driven skyrmion motion propelled by extremely low current density.[5,6] Because skyrmions are recognized as promising candidates to carry information in data storage and logic devices,[7,8] the formation and stability of magnetic skyrmions are an active research area. Experimentally, skyrmions have been observed in materials with chiral-lattice symmetry using neutron scattering[9] and Lorentz microscopy.[10–13] In thin film systems made of non-chiral materials, skyrmions have been observed using spin-polarized scanning tunneling microscopy[14,15] and magneto-optic Kerr microscopy.[16] In most of the reported cases, the emergence of magnetic chirality is attributed to the Dzyaloshinskii-Moriya interaction,[17,18] which arises from inversion symmetry breaking either in the crystal lattice[4–6,9–13] or at interfaces.[15,16,19,20] In general, the simultaneous presence of the Dzyaloshinskii-Moriya interaction and the exchange interaction tends to stabilize extended spin spirals.[21,22] A key question is how the magnetic properties of a system might be modified such that skyrmions can be stabilized[4–6,9–13] and manipulated by means of spin-polarized current.[15,23,24] One approach is to add Zeeman energy by applying an external magnetic field: this can break the symmetry of "up" and "down" domains in spin spirals, resulting in skyrmion formation.[5,6,9–13,15] In some specific systems, such as Fe/Ir(111), four-spin exchange interactions can stabilize skyrmions in the absence of applied magnetic field.[14] Theoretical predictions suggest that the addition of uniaxial anisotropy can stabilize skyrmion phases,[25–28] and planar confinement structures were shown to stabilize skyrmionic vortices.[29–31]

In this letter, we demonstrate the possibility to use interlayer exchange coupling to shift the energy landscape of a chiral spin spiral to stabilize a skyrmion ground state. By using spin polarized low-energy electron microscopy (SPLEEM),[32] we map the spin texture in Fe/Ni bilayers at the top of Fe/Ni/Cu/Ni/Cu(001) structures. The Fe/Ni bilayers are designed so that their magnetic ground state would be a chiral stripe phase (spin spiral) if they were grown directly on the Cu(001) substrate.[33] The Cu/Ni/Cu(001) structure underneath the Fe/Ni films is designed to modify this ground state: the Ni layers have perpendicular magnetic anisotropy and,[34] similar to application of an external magnetic field, exchange coupling through the Cu spacer layer lifts the degeneracy of "up" and "down" domains in the Fe/Ni film on top.[35,36] By tuning the thickness of the Cu interlayer, we find that the spin texture in the Fe/Ni bilayer can be adjusted between single domain, stripe domain, or skyrmion ground states.

The experiments were done using the SPLEEM instrument at Lawrence Berkeley National Laboratory. Cu(001) substrates were cleaned by cycles of Ar^+ sputtering at 1.0 keV and annealing at 580 °C. Ni, Cu, and Fe layers were deposited by electron beam evaporation while substrates were at room temperature, and growth rates were calibrated by measuring oscillation of low-energy electron reflectivity associated with layer-by-layer growth. In all the structures presented in this work, identical Ni base-layers of 15 Monolayer (ML) (here 1 ML is ~1.8 Å (Ref. 37)) thickness were grown first, followed by deposition of Cu spacer layers of varied thickness. The bilayers at the top of the structures are composed of identical Ni layers of 2.0 ML thickness, followed by Fe top layers of varied thicknesses in the range of 2 to 3 ML. To maximize the magnetic contrast, the energy of

[a)]Author to whom correspondence should be addressed. Electronic mail: gchenncem@gmail.com

the incident electron beam was adjusted to 9.2 eV during the growth of Ni and to 5.5 eV during the growth of Fe. After completion of the 15 ML Ni base-layers, the samples were magnetized along the +z out-of-plane direction by applying a 1500 Oe magnetic field. After completion of Fe/Ni/Cu/Ni/Cu(001) multilayers, spin textures were measured by imaging components of the magnetization vector along Cartesian x, y, z directions at room temperature.[33,38–40]

Figure 1 illustrates our approach to stabilize a magnetic skyrmion ground state. Grown directly on a Cu(001) single crystal, the magnetic structure of Fe/Ni bilayer films exhibits a chiral stripe domain phase, this is indicated by red/blue stripes in the sketch in Fig. 1(a).[33] One general property of magnetic stripe domain phases is that, in the presence of external applied magnetic field, transitions to bubble domain ground states tend to occur when the area fraction of up-vs.-down domains is in certain ranges around 70% and 30%;[41,42] the red/blue dotted pattern in the sketch in Fig. 1(b) illustrates this well-known effect. In this letter, we introduce a similar change of the magnetic domain ground state of the Fe/Ni bilayer by applying a *virtual magnetic field* $\vec{H}_{eff}$ that results from the coupling through a non-magnetic Cu spacer layer to a perpendicularly magnetized Ni film,[36] as laid out in Fig. 1(c).

We find a strong influence on the spin textures stabilized in the Fe/Ni bilayers when the Cu spacer layer thickness d_{Cu} is varied in the Fe/Ni/Cu/Ni/Cu(001) multilayers. The SPLEEM results summarized in Fig. 2 show that for $d_{Cu} = 14.6$ ML, Figs. 2(a) and 2(b), the ground state in the FeNi bilayers is a stripe domain phase. Tuning the thickness of the Fe layer d_{Fe} changes the effective out-of-plane anisotropy K,[33,35,36] with a general dependence of $K = K_v d + K_s$,[35,37] where d is film thickness and K_v and K_s are the volume and surface contribution of the anisotropy, respectively. As a result, the width of the stripe domains decreases with increasing d_{Fe}, as the system approaches a spin-reorientation transition to an in-plane magnetized state when d_{Fe} exceeds about 3 ML.[35] In Fig. 2, a ($d_{Fe} = 2.5$ ML) and b ($d_{Fe} = 2.8$ ML), the area fractions of black (down) and white (up) stripe domains are approximately 50%, i.e., up and down domains are energetically degenerate. This indicates that the virtual magnetic field due to interlayer coupling through the $d_{Cu} = 14.6$ ML Cu interlayer to the Ni base-layer

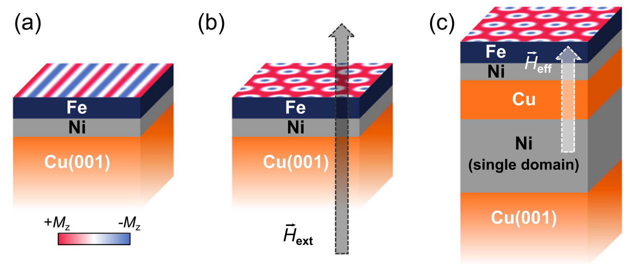

FIG. 1. Sketch of Ni/Fe bilayers. (a) When grown directly on Cu(001) substrates, magnetic stripe domain phases can be stabilized in the absence of external magnetic fields. (b) Transitions from stripe- to magnetic circular domain phases can occur in the presence of external magnetic field $\vec{H}_{ext}$. (c) Our work demonstrates the stabilization of skyrmion ground states by introducing a virtual magnetic field $\vec{H}_{eff}$ by coupling Fe/Ni bilayers to buried single-domain Ni layers.

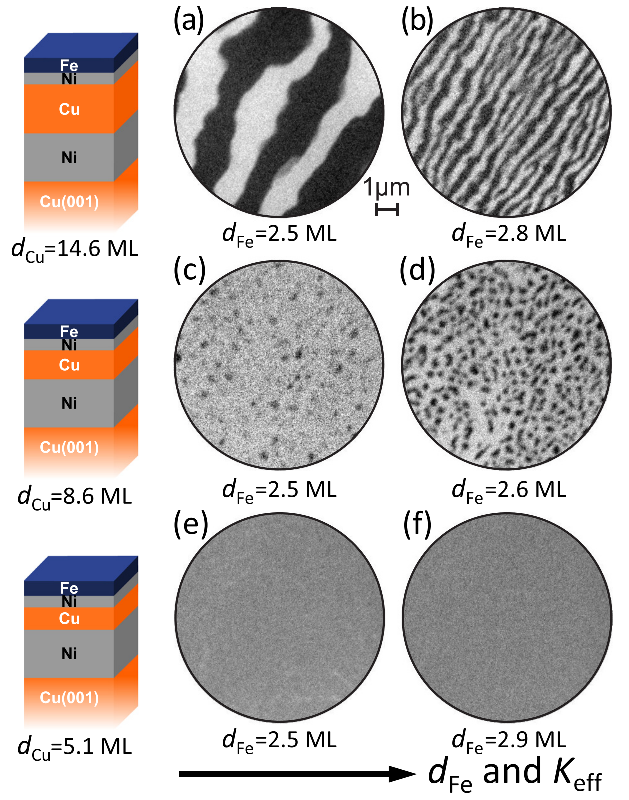

FIG. 2. Selected out-of-plane SPLEEM images of Fe/Ni/Cu/Ni/Cu(001) multilayer structures as sketched on the left. As a function of Cu interlayer thicknesses d_{Cu} of 14.6 ML (top row), 8.6 ML (center row), and 5.1 ML (bottom row), the system forms three different magnetic ground states: (a) and (b) magnetic stripe domain phase, (c) and (d) skyrmion phase, and (e) and (f) single domain states. The different magnetic states are attributed to the different strengths of the virtual magnetic field $\vec{H}_{eff}$, resulting from interlayer exchange coupling between the Fe/Ni bilayer and the buried Ni layer through Cu layers of different thicknesses. Observed changes of spin textures comparing images (a) and (c) versus (b) and (d) are due to variation of the effective out-of-plane anisotropy K_{eff} as a function of the thickness of top Fe layer d_{Fe}.

underneath is negligible compared to the dipolar stray field of the Fe/Ni bilayer.[36,42] The virtual magnetic field changes as a function of the thickness of the Cu interlayer.[35,36] Figs. 2(c) and 2(d) show results for $d_{Cu} = 8.6$ ML, where the stripe domain phase no longer appears. Instead, when the Fe layer thickness is adjusted to approximately $d_{Fe} = 2.5$ ML, ensembles of roughly circular domains with radius around ∼200 nm appear. In this magnetic domain phase, the area fraction of magnetization pointing into the positive z-direction (white) is significantly larger than the area fraction of magnetization pointing in the negative z-direction (black), indicating that the energy of up and down domains is not identical. This lifting of the up/down degeneracy is attributed to interlayer exchange coupling of the Fe/Ni bilayer, through the Cu interlayer, to the Ni base-layer underneath. With the Ni base-layer being magnetized in an out-of-plane single-domain state, this coupling acts as a virtual magnetic field along the out-of-plane direction.[36] This picture can be corroborated by changing the thickness of the Cu interlayer to $d_{Cu} = 5.1$ ML, where the increased strength of the interlayer coupling induces a single domain ground state in the Fe/Ni bilayer, as shown in Figs. 2(e) and 2(f). This observed d_{Cu} dependent evolution of domain states is analogous to the emergence of spin spirals, skyrmions, and single domain states in the experimental observation in helical magnets[5,6,9–13] or cycloidal magnets,[15,16] and in Monte-Carlo simulation[43] in the presence of external magnetic field.

Skyrmions are categorized by their non-trivial topological properties such as hedgehog or spiral texture and winding number. In the following, we characterize the topology of the small circular shaped domains that emerge in these Fe/Ni/Cu/Ni/Cu(001) multilayers, as observed in Figs. 2(c) and 2(d). We use the SPLEEM to image three dimensional spin textures: first, triplets of SPLEEM images are acquired with the spin polarization of the electron beam oriented along Cartesian directions, to image the x, y, and z components of the magnetization independently. Then, color-coded compound images are constructed to resolve orientation of the magnetization vector across the field of view. An example is shown in Fig. 3(a) where, in each image pixel, gray-scale represents the magnetization component along the surface normal directions (+z/light and −z/dark) and the magnetization component along in-plane directions (x, y) is represented in colors corresponding to the hue-saturation-lightness color wheel shown in the inset. The small circular shaped domains all share the same magnetization texture: in the surrounding area magnetization points up (+z/light), in the center of the circular domains magnetization points down (−z/dark), and in the perimeter regions the magnetization vector points towards the domain centers. The perimeters are thus right-handed chiral cycloidal-, or, Néel-textures,[33,38] and thus these magnetization features can be described as right-handed hedgehog skyrmions with winding number 1.

The chirality of these magnetic features can be analyzed more quantitatively by measuring the statistical distribution of magnetization directions as a function of location with respect to skyrmion centers.[38–40] We can start by defining equatorial lines for each skyrmion as the lines circling around the skyrmion cores where the magnetization is fully in-plane (i.e., where the out-of plane component of **m** vanishes). In each pixel on these skyrmion equators, we measure the in-plane orientation of the magnetization vector **m** and the orientation of the normal vector **n** of the skyrmion equator (to avoid ambiguity, we define **n** to point away from the skyrmion cores). Figure 3(b) plots a histogram of the angle α measured between the magnetization vector **m** and normal vector **n** of the skyrmion equators in all skyrmions observed in Fig. 3(a). The histogram shows that measurements of the angle α are strongly peaked at 180°, confirming the qualitative designation of these features as right-handed Néel-type.[38–40] The analysis of images of several samples (not shown) corroborates that this right-handed Néel-texture is a reproducible feature of the Fe/Ni/Cu/Ni/Cu(001) system.

For a more detailed description of the spin texture of these skyrmions across their surfaces, we focus on one single skyrmion with radius of approximately 200 nm. Figure 3(c) shows a magnified color-coded compound SPLEEM image. Fig. 3(d) shows how the inclination of the magnetization vector with respect to the surface normal reverses with increasing distance from the center of the skyrmion. As a function of distance r from the skyrmion center, the angle θ between the magnetization **m** and the surface normal

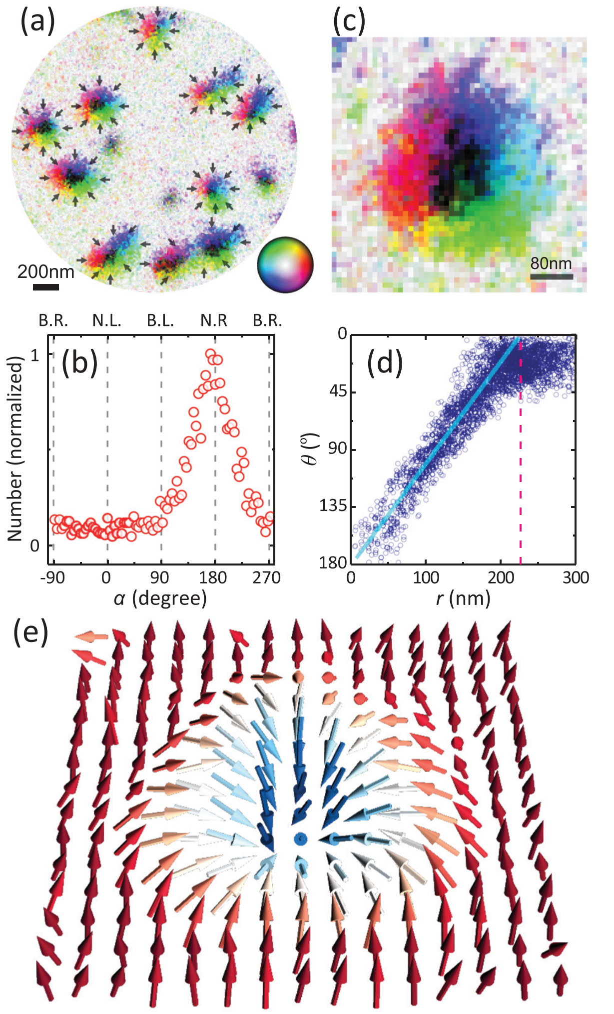

FIG. 3. Room temperature skyrmion phase in the top-most Fe/Ni bilayer of the multilayer structure sketched in Figure 1(c), Fe(2.5)/Ni(2)/Cu(8.4)/Ni(15)/Cu(001). (a) SPLEEM image plots 3D magnetization vector components of skyrmions according to color-wheel shown in the inset. Additionally, black arrows highlight skyrmion perimeter magnetization directions. (b) Histogram of magnetization angle measurements taken in skyrmion perimeters of data from panel (a). This histogram shows that the skyrmion type is right-handed cycloidal (Néel). (c) Magnified image of a single skyrmion. (d) Pixel-by-pixel measurement of the angle θ between magnetization and the (001) surface normal, as a function of distance r from skyrmion centers. (e) Arrows-array representation of the experimental data shown in panel (c). The orientation of arrows shows magnetization vector direction of cells averaged from 3 × 3 pixels in the original data.

direction (001) tilts smoothly in almost linear proportion to r (blue circle symbols are pixel-by-pixel measurements, and cyan solid line is a guide to the eye). The linear dependence of θ on r suggests that the imaged spin-textures are minimal-size skyrmions of this system, consistent with theoretical calculations,[44,45] as opposed to bubble domains. In the latter case, the $\theta(r)$ diagram would be expected to be non-linear, featuring an area of constant out-of-plane magnetization, $\theta = -180°$, near the domain center and extending to some distance $r > 0$. The slope of the $\theta(r)$ measurement shows that the spin rotates by ~0.8° per nm, that is, around 0.14° between two neighboring atoms. To display the measured spin texture more clearly, the array of vectors shown in Fig. 3(e) illustrates the same data as the compound SPLEEM image from Fig. 3(c). Here, arrows show the magnetization direction of cells averaged from 3 × 3 pixels in the original data, highlighting the measured spin texture of this hedgehog skyrmion.

The type of magnetization textures described in this letter is also consistent with the previous experimental observation on Fe/Ni/Cu(001) bilayers,[33] where the origin of the right-handed Néel-type chirality was attributed to interfacial Dzyaloshinskii-Moriya interaction.[17,18,20] Magnetic chirality of this type of multilayer structures is robust within a certain range of film thicknesses, which is determined by the interplay between the dipolar energy (related to the film thickness) and the strength of the interfacial Dzyaloshinskii-Moriya interaction.[33,38] In addition, the stability of homochiral magnetization textures can be extended to thicker films by growing ternary superlattices.[39] We also note that such Néel-type skyrmions in multilayer systems[14–16] are different from Bloch-type (helical) skyrmions observed in B20 materials.[6,10–13] This difference can be understood by recalling that the energy term of the Dzyaloshinskii–Moriya interaction is $E = -\boldsymbol{D}_{ij} \cdot (\boldsymbol{S}_i \times \boldsymbol{S}_j)$, where $\mathbf{D}_{ij}$ is the Dzyaloshinskii–Moriya interaction vector, and $\boldsymbol{S}_i$ and $\boldsymbol{S}_j$ are spins at two neighboring sites i and j. Moriya's model[8,18,20] indicates that in thin film systems, the Dzyaloshinskii–Moriya vector $\mathbf{D}_{ij}$ at sites i and j is usually perpendicular to the distance vector $\mathbf{r}_{ij}$ between the sites. In contrast, $\mathbf{D}_{ij}$ is parallel to $\mathbf{r}_{ij}$ in B20 structures.[8,10,18] The different orientation of $\mathbf{D}_{ij}$ causes the Néel- vs. Bloch-type spin textures in thin film vs. B20 systems through the energy term of the Dzyaloshinskii–Moriya interaction. We also point out that the skyrmion ensembles in the Fe/Ni/Cu/Ni/Cu(001) multilayers were not observed to form periodically ordered arrays, as found in theoretical results[7,41] and in skyrmions observed in bulk materials and much thicker films.[5–13] One may speculate that the lack of ordering could be due to pinning associated with defects or roughness of the Cu(001) substrate or interfaces within the multilayers.[36,42] Further work is required to determine whether more regular skyrmion arrays might be found as fabrication of the multilayer structures is modified.[39,45]

To conclude, we have imaged the spin textures in the Fe/Ni/Cu/Ni/Cu(001) system using SPLEEM. We found that tuning the thickness of a Cu spacer layer allows us to tailor the magnitude of a virtual magnetic field through interlayer coupling. This approach is shown to shift the energy landscape in the Fe/Ni bilayers at the top of the structures to stabilize ambient-temperature skyrmion ground states. These results may be helpful for the design of skyrmion based spintronics devices.

Experiments were performed at the Molecular Foundry, Lawrence Berkeley National Laboratory, supported by the Office of Science, Office of Basic Energy Sciences, Scientific User Facilities Division, of the U.S. Department of Energy under Contract No. DE-AC02—05CH11231. A.M. thanks the Spanish Minister of Education for support under Grant No. PRX14/00307.

[1] T. H. R. Skyrme, Nucl. Phys. **31**, 556 (1962).
[2] A. Bogdanov and A. Hubert, J. Magn. Magn. Mater. **138**, 255 (1994).
[3] U. K. Roszler, A. N. Bogdanov, and C. Pfleiderer, Nature (London) **442**, 797 (2006).
[4] A. Neubauer, C. Pfleiderer, B. Binz, A. Rosch, R. Ritz, P. G. Niklowitz, and P. Böni, Phys. Rev. Lett. **102**, 186602 (2009).
[5] F. Jonietz, S. Mühlbauer, C. Pfleiderer, A. Neubauer, W. Münzer, A. Baufer, T. Adams, R. Georgii, P. Böni, R. A. Duine *et al.*, Science **330**, 1648 (2010).
[6] X. Z. Yu, N. Kanazawa, W. Z. Zhang, T. Nagai, T. Hara, K. Kimoto, Y. Matsui, Y. Onose, and Y. Tokura, Nat. Commun. **3**, 988 (2012).
[7] N. Nagaosa and Y. Tokura, Nat. Nanotechnol. **8**, 899 (2013).
[8] A. Fert, V. Cros, and J. Sampaio, Nat. Nanotechnol. **8**, 152 (2013).
[9] S. Mühlbauer, B. Binz, F. Jonietz, C. Pfleiderer, A. Rosch, A. Neubauer, R. Georgii, and P. Böni, Science **323**, 915 (2009).
[10] X. Z. Yu, Y. Onose, N. Kanazawa, J. H. Park, J. H. Han, Y. Matsui, N. Nagaosa, and Y. Tokura, Nature (London) **465**, 901 (2010).
[11] X. Z. Yu, N. Kanazawa, Y. Onose, K. Kimoto, W. Z. Zhang, S. Ishiwata, Y. Matsui, and Y. Tokura, Nat. Mater. **10**, 106 (2011).
[12] S. Seki, X. Z. Yu, S. Ishiwata, and Y. Tokura, Science **336**, 198 (2012).
[13] Y. Li, N. Kanazawa, X. Z. Yu, A. Tsukazaki, M. Kawasaki, M. Ichikawa, X. F. Jin, F. Kagawa, and Y. Tokura, Phys. Rev. Lett. **110**, 117202 (2013).
[14] S. Heinze, K. von Bergmann, M. Menzel, J. Brede, A. Kubetzka, R. Wiesendanger, G. Bihlmayer, and S. Blügel, Nat. Phys. **7**, 713 (2011).
[15] N. Romming, C. Hanneken, M. Menzel, J. E. Bickel, B. Wolter, K. von Bergmann, A. Kubetzka, and R. Wiesendanger, Science **341**, 636 (2013).
[16] W. Jiang, P. Upadhyaya, W. Zhang, G. Yu, M. Benjamin Jungfleisch, F. Y. Fradin, J. E. Pearson, Y. Tserkovnyak, K. L. Wang, O. Heinonen, S. G. E. te Velthuis, and A. Hoffmann, e-print arXiv:1502.08028 [cond-mat.mtrl-sci].
[17] I. Dzyaloshinsky, J. Phys. Chem. Solids **4**, 241 (1958).
[18] T. Moriya, Phys. Rev. **120**, 91 (1960).
[19] A. Fert, Mater. Sci. Forum **59–60**, 439 (1990).
[20] A. Crépieux and C. Lacroix, J. Magn. Magn. Mater. **182**, 341 (1998).
[21] M. Uchida, Y. Onose, Y. Matsui, and Y. Tokura, Science **311**, 359 (2006).
[22] M. Bode, M. Heide, K. von Bergmann, P. Ferriani, S. Heinze, G. Bihlmayer, A. Kubetzka, O. Pietzsch, S. Blügel, and R. Wiesendanger, Nature **447**, 190 (2007).
[23] J. Iwasaki, M. Mochizuki, and N. Nagaosa, Nat. Nanotechnol. **8**, 742 (2013).
[24] J. Sampaio, V. Cros, S. Rohart, A. Thiaville, and A. Fert, Nat. Nanotechnol. **8**, 839 (2013).
[25] A. B. Butenko, A. A. Leonov, U. K. Rößler, and A. N. Bogdanov, Phys. Rev. B **82**, 052403 (2010).
[26] N. S. Kiselev, A. N. Bogdanov, R. Schäfer, and U. K. Rößler, J. Phys. D: Appl. Phys. **44**, 392001 (2011).
[27] E. A. Karhu, U. K. Rößler, A. N. Bogdanov, S. Kahwaji, B. J. Kirby, H. Fritzsche, M. D. Robertson, C. F. Majkrzak, and T. L. Monchesky, Phys. Rev. B **85**, 094429 (2012).
[28] M. N. Wilson, E. A. Karhu, A. S. Quigley, U. K. Rößler, A. B. Butenko, A. N. Bogdanov, M. D. Robertson, and T. L. Monchesky, Phys. Rev. B **86**, 144420 (2012).
[29] L. Sun, R. X. Cao, B. F. Miao, Z. Feng, B. You, D. Wu, W. Zhang, A. Hu, and H. F. Ding, Phys. Rev. Lett. **110**, 167201 (2013).
[30] J. Li, A. Tan, K. W. Moon, A. Doran, M. A. Marcus, A. T. Young, E. Arenholz, S. Ma, R. F. Yang, C. Hwang, and Z. Q. Qiu, Nat. Commun. **5**, 4704 (2014).
[31] B. F. Miao, L. Sun, Y. W. Wu, X. D. Tao, X. Xiong, Y. Wen, R. X. Cao, P. Wang, D. Wu, Q. F. Zhan, B. You, J. Du, R. W. Li, and H. F. Ding, Phys. Rev. B **90**, 174411 (2014).
[32] N. Rougemaille and A. K. Schmid, Eur. Phys. J.: Appl. Phys. **50**, 20101 (2010).
[33] G. Chen, J. Zhu, A. Quesada, J. Li, A. T. N'Diaye, Y. Huo, T. P. Ma, Y. Chen, H. Y. Kwon, C. Won, Z. Q. Qiu, A. K. Schmid, and Y. Z. Wu, Phys. Rev. Lett. **110**, 177204 (2013).
[34] B. Schulz and K. Baberschke, Phys. Rev. B **50**, 13467 (1994).
[35] Y. Z. Wu, C. Won, A. Scholl, A. Doran, H. W. Zhao, X. F. Jin, and Z. Q. Qiu, Phys. Rev. Lett. **93**, 117205 (2004).
[36] J. Wu, J. Choi, C. Won, Y. Z. Wu, A. Scholl, A. Doran, C. Hwang, and Z. Q. Qiu, Phys. Rev. B **79**, 014429 (2009).
[37] C. Won, Y. Z. Wu, J. Choi, W. Kim, A. Scholl, A. Doran, T. Owens, J. Wu, X. F. Jin, H. W. Zhao, and Z. Q. Qiu, Phys. Rev. B **71**, 224429 (2005).
[38] G. Chen, T. Ma, A. T. N'Diaye, H. Kwon, C. Won, Y. Wu, and A. K. Schmid, Nat. Commun. **4**, 2671 (2013).
[39] G. Chen, A. T. N'Diaye, Y. Wu, and A. K. Schmid, Appl. Phys. Lett. **106**, 062402 (2015).

[40]G. Chen, A. T. N'Diaye, S. P. Kang, H. Y. Kwon, C. Won, Y. Wu, Z. Q. Qiu, and A. K. Schmid, Nat. Commun. **6**, 6598 (2015).
[41]K.-O. Ng and D. Vanderbilt, Phys. Rev. B **52**, 2177 (1995).
[42]N. Saratz, A. Lichtenberger, O. Portmann, U. Ramsperger, A. Vindigni, and D. Pescia, Phys. Rev. Lett. **104**, 077203 (2010).
[43]H. Y. Kwon and C. Won, J. Magn. Magn. Mater. **351**, 8 (2014).
[44]J. Hoon Han, J. Zang, Z. Yang, J.-H. Park, and N. Nagaosa, Phys. Rev. B **82**, 094429 (2010).
[45]B. Dupé, G. Bihlmayer, S. Blügel, and S. Heinze, e-print arXiv:1503.08098 [cond-mat.mtrl-sci].